IEICE TRANS. COMMUN., VOL.E89–B, NO.1 JANUARY 2006

PAPER

Frequency-Domain Pre-Equalization for MC-CDMA/TDD Uplink and Its Bit Error Rate Analysis

Satoshi ABE[†a)], ***Member***, **Shinsuke TAKAOKA**[†], **Hiromichi TOMEBA**[†], ***Student Members***, ***and*** **Fumiyuki ADACHI**[†], ***Member***

SUMMARY In multi-carrier code division multiple access (MC-CDMA) uplink (mobile-to-base station), since different users' signals go through different frequency-selective fading channels, large multi-access interference (MAI) is produced. The use of frequency-domain equalization reception can only partially restore the orthogonality among different users' signals, resulting in a severe degradation in the bit error rate (BER) performance. Hence, frequency-domain pre-equalization transmission, which equalizes the MC-CDMA signal before transmission, is recently attracting attention. In this paper, we present a generalized minimum mean square error (GMMSE) frequency-domain pre-equalization transmission suitable for MC-CDMA/TDD uplink. The pre-equalization weight is derived based on the method of Lagrange multipliers. The theoretical analysis of BER performance using the GMMSE frequency-domain pre-equalization transmission in a frequency-selective Rayleigh fading channel is presented and the result is confirmed by computer simulation.

key words: *MC-CDMA, frequency-domain pre-equalization, frequency-selective channel*

1. Introduction

In next-generation mobile communications systems, high-speed and high-quality data communications services will be demanded. However, in high-speed data communications, the bit error rate (BER) performance significantly degrades due to severe inter-symbol interference (ISI) produced by frequency-selective fading [1]. Recently, multi-carrier code division multiple access (MC-CDMA) has been attracting much attention as a promising candidate for multi-access technique [2], [3]. In MC-CDMA, frequency-domain spreading is used, where each data symbol to be transmitted is spread over a number of orthogonal subcarriers (on the other hand, time-domain spreading is used in direct sequence CDMA (DS-CDMA)). Using frequency-domain equalization reception, MC-CDMA can exploit the channel frequency-selectivity to improve the downlink BER performance [2]–[4]. However, in the MC-CDMA uplink, since different users' signals go through different frequency-selective fading channels, the use of frequency-domain equalization reception can only partially restore the orthogonality among different users' signals and thus, the multi-access interference (MAI) still remains, resulting in a degraded performance [2].

Manuscript received February 14, 2005.
Manuscript revised July 7, 2005.

[†]The authors are with the Department of Electrical and Communication Engineering, Graduate School of Engineering, Tohoku University, Sendai-shi, 980-8579 Japan.
a) E-mail: abe@mobile.ecei.tohoku.ac.jp

DOI: 10.1093/ietcom/e89–b.1.162

Multiuser detection can be used to reduce the MAI [5]. However, if the maximum likelihood multiuser detection is used, the receiver complexity grows exponentially as the number of users increases. Interference cancellation, which makes tentative decision on each user's data and subtracts them from the received signal, requires the knowledge of all users' spreading codes and channels at a base station (BS). Multi-stage interference canceller can improve the performance, but it has a longer processing delay.

MAI is produced due to the orthogonality distortion resulting from the non-flat transfer function of the channel (i.e., a frequency-selective channel). MAI can be mitigated if each user's channel is transformed into a frequency-nonselective channel by using frequency-domain pre-equalization that uses pre-equalization weight which is inversely proportional to the channel transfer function. Such equalization is called zero forcing (ZF) frequency-domain pre-equalization. However, if ZF pre-equalization is used, the transmit power must be significantly increased at subcarriers where the channel gain drops. If the total transmit power is kept the same as before pre-equalization, then a large power loss in the received signal is produced. This means that the BER performance achievable with ZF pre-equalization at a given transmit power degrades significantly. Hence, frequency-domain pre-equalization which suppresses MAI while reducing the power loss is necessary. Recently, frequency-domain pre-equalization was proposed for MC-CDMA [6]. In Ref. [6], several pre-equalization techniques with the total transmit power constraints are presented. The best BER performance is obtained by the quasi-minimum mean square error (quasi-MMSE) pre-equalization (this is shown in Sect. 5.6).

In this paper, we propose a new frequency-domain pre-equalization, based on a different method from Ref. [6], for an MC-CDMA/time-division-duplex (TDD) system and show that almost the same BER performance can be achieved as using the quasi-MMSE pre-equalization technique of Ref. [6]. In the proposed pre-equalization method, the equalization target is introduced and the pre-equalization weight is determined so that the mean square error (MSE) between the equivalent channel gain and the prescribed target value is minimized under the total transmit power constraint, thereby restoring the orthogonality property among users to minimize the MAI. The pre-equalization weight is computed by using the method of Lagrange multipliers [8]. The proposed pre-equalization method is called a general-

Copyright © 2006 The Institute of Electronics, Information and Communication Engineers

ized MMSE (GMMSE) frequency-domain pre-equalization in this paper.

The rest of the paper is organized as follows. In Sect. 2, MC-CDMA/TDD transmission model is presented. The principle operation of the GMMSE frequency-domain pre-equalization is presented in Sect. 3. In Sect. 4, the theoretical analysis of the conditional BER for the MC-CDMA/TDD uplink with GMMSE frequency-domain pre-equalization is presented. In Sect. 5, the theoretical average BER performance is numerically evaluated by Monte Carlo numerical method and is confirmed by computer simulation. The average BER performance achievable with the GMMSE pre-equalization is compared with those of various frequency-domain pre-equalizations presented in Ref. [6]. Finally, Sect. 6 concludes the paper.

2. MC-CDMA/TDD Transmission Model

TDD is considered as a promising duplex method for the next-generation high-speed mobile communications [7]. The TDD frame structure is illustrated in Fig. 1, where the same carrier frequency is used alternately for downlink (DL) and uplink (UL) transmissions. Since the downlink and uplink time slots are short enough in high-speed data communications, the channel gains can be assumed to be almost constant over at least one frame and therefore, the pre-equalization weights for the uplink can be computed by using the downlink channel estimate. However, in this paper, ideal channel estimation is assumed. It is also assumed that the distance dependant path loss and shadowing loss are completely regulated by ideal slow transmit power control (TPC). However, even if close-to-frequency-nonselective channel can be achieved by pre-equalization, the orthogonality among different users is lost if all users' signals received at the BS are not time-synchronous. In this paper, the impact of the timing error is discussed in Sect. 5.7.

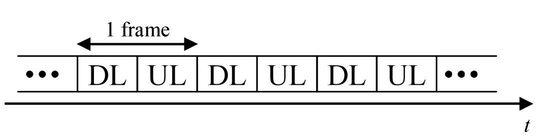

Fig. 1 TDD frame structure.

Transmitter/receiver structure of the uth user for MC-CDMA/TDD using GMMSE frequency-domain pre-equalization is illustrated in Fig. 2. We assume an MC-CDMA using N subcarriers. At the downlink receiver, the received MC-CDMA downlink signal is decomposed into N subcarrier components after the removal of guard interval (GI) and then, channel estimation and frequency-domain equalization are carried out, followed by despreading and data-demodulation. At the uplink transmitter, a binary transmit data sequence is transformed into data-modulated symbol sequence, which is spread by an orthogonal spreading sequence and then, multiplied by a scramble sequence common to all users. After serial-to-parallel (S/P) conversion to N streams, frequency-interleaving is applied in order to achieve larger frequency diversity effect even for a small spreading factor (subcarriers belonging to the same data symbol are separated enough to experience independent fading). Then, pre-equalization is carried out (pre-equalization weight is computed using the downlink channel estimate). Finally N-point inverse FFT (IFFT) is applied to transform the spread signal into a pre-equalized MC-CDMA signal, followed by the GI insertion.

2.1 Transmit Signal

We consider the transmission of N/SF data modulated symbols during one MC-CDMA signaling period, where SF is the spreading factor. Quadrature phase shift keying (QPSK) data-modulated symbol sequence $\{d_u(i);\, i = 0 \sim N/SF - 1\}$ of the uth user is spread by the orthogonal spreading sequence $\{c_u(n' \bmod SF);\, n' = 0 \sim N - 1\}$ and multiplied by the common scramble sequence $\{c_{scr}(n');\, n' = 0 \sim N - 1\}$. Then, the resultant chip sequence is S/P converted to map each chip onto a different subcarrier. The n'th subcarrier component $S_u(n')$ can be expressed as

$$S_u(n') = \sqrt{\frac{2E_t}{T_c}\frac{1}{SF \cdot N}}\, c_u(n' \bmod SF)\, c_{scr}(n') d_u\left(\left\lfloor \frac{n'}{SF} \right\rfloor\right), \qquad (1)$$

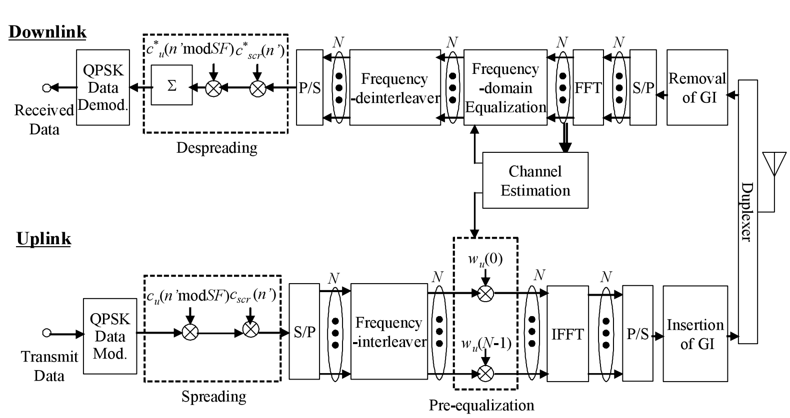

Fig. 2 Transmitter/receiver structure of the uth user for MC-CDMA/TDD.

where E_t denotes the transmit symbol energy, T_c the IFFT sampling period, and $\lfloor x \rfloor$ the largest integer smaller than or equal to x. Then, frequency-interleaving is applied. In this paper, an $SF \times N/SF$ block interleaver is used. By applying this interleaving, the n'th subcarrier component is mapped to the nth subcarrier as

$$n = (n' \bmod SF) \times SF + \left\lfloor \frac{n'}{SF} \right\rfloor. \tag{2}$$

Then each subcarrier component is multiplied by the pre-equalization weight $w_u(n)$ (the derivation of $w_u(n)$ is presented in Sect. 3). After applying N-point IFFT and inserting the N_g-sample GI, the pre-equalized MC-CDMA signal $s_u(t)$ is transmitted. In this paper, a T_c-spaced discrete-time representation of the signal is used. $s_u(t)$ can be expressed, using the equivalent baseband representation, as

$$\begin{aligned} s_u(t) &= \sum_{n=0}^{N-1} S_u(n) w_u(n) \exp\left(j2\pi n \frac{t}{N}\right), \\ t &= -N_g \sim N-1. \end{aligned} \tag{3}$$

2.2 Channel Model

A frequency-selective block fading channel having T_c-spaced L discrete paths is assumed. The block fading assumption means that the path gains stay constant over one MC-CDMA signaling interval of $t = -N_g \sim N-1$. Let the complex path gain and time delay of the lth path between the uth user and a base station be $\xi_{u,l}$ and $\tau_{u,l}$, respectively, where $\tau_{u,l} \le N_g - 1$ and $\sum_{l=0}^{L-1} E\left[\left|\xi_{u,l}\right|^2\right] = 1$; $E[.]$ is the ensemble average operation. The received signal $r(t)$ can be expressed as

$$\begin{aligned} r(t) &= \sum_{u=0}^{U-1} \sum_{l=0}^{L-1} \xi_{u,l} s_u(t - \tau_{u,l}) + \eta(t), \\ t &= -N_g \sim N-1, \end{aligned} \tag{4}$$

where U represents the number of users, $\eta(t)$ is the complex Gaussian noise with zero mean and variance $2N_0/T_c$, and N_0 represents the single-sided power spectrum density of the additive white Gaussian noise (AWGN).

2.3 Received Signal

At a base station receiver, after removing the GI, FFT is applied to decompose the received signal $\{r(t); t = 0 \sim N-1\}$ into N subcarrier components. The nth subcarrier component $R(n)$ can be expressed as

$$\begin{aligned} R(n) &= \frac{1}{N} \sum_{t=0}^{N-1} r(t) \exp\left(-j2\pi n \frac{t}{N}\right) \\ &= \sum_{u=0}^{U-1} S_u(n) \hat{H}_u(n) + \Pi(n), \end{aligned} \tag{5}$$

where

$$\hat{H}_u(n) = H_u(n) w_u(n), \tag{6}$$

is the equivalent channel gain seen at the base station with $H_u(n)$ being the uth user's channel gain at the nth subcarrier and $\Pi(n)$ is the noise component due to the AWGN. They are given by

$$\begin{cases} H_u(n) = \displaystyle\sum_{l=0}^{L-1} \xi_{u,l} \exp\left(-j2\pi n \frac{\tau_{u,l}}{N}\right) \\ \Pi(n) = \displaystyle\frac{1}{N} \sum_{t=0}^{N-1} \eta(t) \exp\left(-j2\pi n \frac{t}{N}\right) \end{cases}. \tag{7}$$

After parallel-to-serial (P/S) conversion, frequency-deinterleaving is applied and the nth subcarrier is demapped to the n'th subcarrier as

$$n' = (n \bmod (N/SF)) \times N/SF + \left\lfloor \frac{n}{N/SF} \right\rfloor. \tag{8}$$

Then, the decision variable $\hat{d}_u(i)$, associated with the ith transmitted data symbol $d_u(i)$, is obtained by despreading as

$$\hat{d}_u(i) = \frac{1}{SF} \sum_{n'=iSF}^{(i+1)SF-1} R(n) c_u^*(n' \bmod SF) c_{scr}^*(n'), \tag{9}$$

where * denotes the complex conjugate operation. Data demodulation is carried out using $\hat{d}_u(i)$.

3. Generalized MMSE Frequency-Domain Pre-Equalization

3.1 Pre-Equalization Weight

In GMMSE frequency-domain pre-equalization, the equalization weight $w_u(n)$ is determined so that the mean square error between the equivalent channel gain $\hat{H}_u(n)$ and the equalization target x is minimized under the transmit power constraint as

$$\begin{aligned} &\text{minimize} \quad e^2 = \frac{1}{N} \sum_{n=0}^{N-1} \left|\hat{H}_u(n) - x\right|^2 \\ &\text{subject to} \quad \frac{1}{N} \sum_{n=0}^{N-1} |w_u(n)|^2 = 1. \end{aligned} \tag{10}$$

By using the method of Lagrange multipliers [8], $w_u(n)$ can be obtained as

$$w_u(n) = \frac{x H_u^*(n)}{|H_u(n)|^2 + \lambda_u}, \tag{11}$$

where λ_u is the controling parameter, which should satisfy

$$\sum_{n=0}^{N-1} \left(\frac{|H_u(n)|}{|H_u(n)|^2 + \lambda_u^2} \right)^2 = \frac{N}{x^2} \tag{12}$$

and can be found by numerical computation.

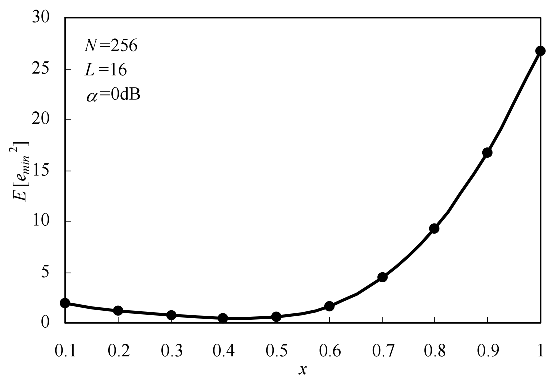

Fig. 3 Pre-equalization error.

3.2 Pre-Equalization Target x and Pre-Equalization Error

The relationship between the pre-equalization target x and the pre-equalization error is discussed below. For simplicity, we assume U=1 and $S(n)$=1, and neglect the noise effect. The ensemble average $E[e^2_{\min}]$ of the minimum mean square error $e^2_{\min}$ is plotted as a function of the equalization target x in Fig. 3. As x reduces from 1, the pre-equalization error decreases and approaches its minimum. However, the pre-equalization error starts to increase when x becomes less than 0.5. The pre-equalization weight amplitude $|w(n)|$ and the equivalent channel gain amplitude $\left|\hat{H}(n)\right|$ seen at the base station are shown for x=0.1, 0.5 and 1 in Fig. 4. When x=1, $|w(n)|$ is almost inversely proportional to $|H(n)|$. However, the pre-equalization weight becomes small for the subcarrier at which the channel gain experiences deep fade. This is because of the total transmit power constraint and thus, the equivalent channel gain cannot be made completely flat. On the other hand, if small x is used (e.g., x=0.1 and 0.5), since the power constraint with respect to λ_u becomes loose (see Eq. (12)), the equivalent channel gain becomes almost flat as seen in Fig. 4(b). However, the averaged equivalent channel gain reduces (resulting in the power loss in the received signal).

It can be seen from Fig. 3 that the optimum x that minimizes the pre-equalization error is around x=0.4~0.5. If x=0.4~0.5 is used, the MAI can be significantly reduced, since the orthogonality property among users can be restored to some extent while avoiding the power loss. Therefore, when the number U of users is large and the MAI is the dominant cause of errors, the uplink BER performance can be improved. However, if too small x is used (e.g., x=0.1), a large power loss occurs in the received signal and the predominant cause of error becomes the noise due to the AWGN. This may cause and the BER performance to degrade. Hence, the orthogonality restoration and the received signal power loss are in the trade-off relationship. Since the optimum x depends on the channel frequency-selectivity and the transmit signal power-to-noise ratio, it is quite difficult to theoretically find the optimum x if not impossible and therefore, we resort to the computer simulation for this problem.

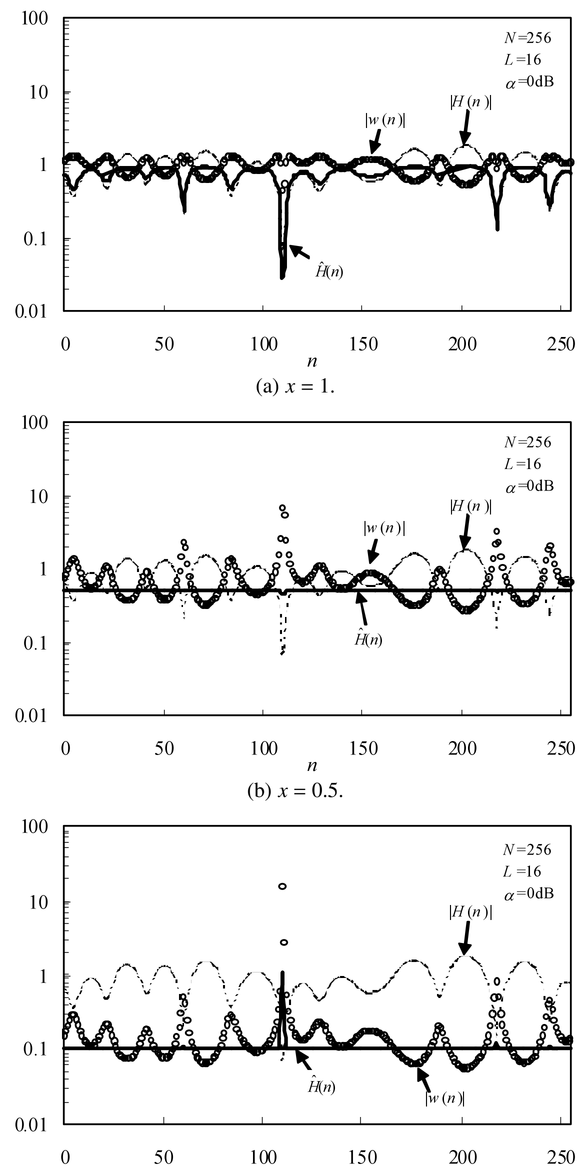

(a) x = 1.

(b) x = 0.5.

(c) x = 0.1.

Fig. 4 Pre-equalization weight and equivalent channel gain.

4. BER Analysis for QPSK Data-Modulation

The conditional BER for the given set of $\{H_u(n);\ n = 0 \sim N-1, u = 0 \sim U-1\}$ is derived for QPSK data-modulation.

Substituting Eqs. (1) and (5) into Eq. (9), we obtain

$$\hat{d}_u(i) = \sqrt{\frac{2E_t}{T_c}\frac{1}{SF \cdot N}}d_u(i)\left(\frac{1}{SF}\sum_{n'=iSF}^{(i+1)SF-1}\hat{H}_u(n)\right) + \mu_{MAI}(i) + \mu_{AWGN}(i), \tag{13}$$

where n is given by Eq. (2) and $\mu_{MAI}(i)$ and $\mu_{AWGN}(i)$ are the MAI and noise components, respectively, and are given by

$$\begin{cases} \mu_{MAI}(i) = \sqrt{\frac{2E_t}{T_c}\frac{1}{SF\cdot N}} \\ \quad \times \sum_{\substack{u'=0\\ \neq u}}^{U-1} d_{u'}(i)\left(\frac{1}{SF}\sum_{n'=iSF}^{(i+1)SF-1}\left\{\begin{array}{l}\hat{H}_{u'}(n)c_{u'}(n' \bmod SF)\\ \times c_u^*(n' \bmod SF)\end{array}\right\}\right) \\ \mu_{AWGN}(i) = \frac{1}{SF}\sum_{n'=iSF}^{(i+1)SF-1}\Pi(n)c_u^*(n' \bmod SF)\end{cases} \tag{14}$$

It is understood from Eq. (13) that $\hat{d}_u(i)$ is a random variable with mean $\sqrt{\frac{2E_t}{T_c}\frac{1}{SF\cdot N}}d_u(i)\left(\frac{1}{SF}\sum_{n'=iSF}^{(i+1)SF-1}\hat{H}_u(n)\right)$. Approximating the MAI component as a zero-mean complex Gaussian process, the sum of $\mu_{MAI}(i)$ and $\mu_{AWGN}(i)$ can be treated as a new, zero-mean complex Gaussian process $\mu(i)$. Since $\mu_{MAI}(i)$ and $\mu_{AWGN}(i)$ are independent, the variance $2\sigma_\mu^2$ of $\mu(i)$ is given by

$$2\sigma_\mu^2 = E\left[|\mu(i)|^2\right] = 2\sigma_{MAI}^2 + 2\sigma_{AWGN}^2, \tag{15}$$

where $2\sigma_{MAI}^2$ and $2\sigma_{AWGN}^2$ are respectively the variances of $\mu_{MAI}(i)$ and $\mu_{AWGN}(i)$. From Eq. (14), σ_μ^2 is given by (see Appendix A)

$$\sigma_\mu^2 = \frac{N_0}{NT_c}\frac{1}{SF} \times \left[\begin{array}{l} 1+\frac{1}{SF}\frac{E_t}{N_0} \\ \quad \times \sum_{\substack{u'=0\\ \neq u}}^{U-1}\left\{\frac{1}{SF}\sum_{n'=iSF}^{(i+1)SF-1}\left|\hat{H}_{u'}(n)\right|^2 \right. \\ \quad \left. -\left|\frac{1}{SF}\sum_{n'=iSF}^{(i+1)SF-1}\hat{H}_{u'}(n)\right|^2\right\}\end{array}\right]. \tag{16}$$

The conditional BER of QPSK data-modulation for the given set of $\{H_u(n); n = 0 \sim N-1, u = 0 \sim U-1\}$ is given by [9]

$$p_b\left(\frac{E_t}{N_0},\{H_u(n)\}\right) = \frac{1}{2}erfc\left[\sqrt{\frac{1}{4}\gamma\left(\frac{E_t}{N_0},\{H_u(n)\}\right)}\right], \tag{17}$$

where $erfc[x] = \left(2/\sqrt{\pi}\right)\int_x^\infty \exp(-t^2)dt$ represents the complementary error function and $\gamma(E_t/N_0, \{H_u(n)\})$ is the instantaneous received signal-to-interference plus noise power ratio (SINR), given by

$$\gamma\left(\frac{E_t}{N_0},\{H_u(n)\}\right) = \frac{\left(\sqrt{\frac{2E_t}{T_c}\frac{1}{SF\cdot N}}\frac{1}{SF}\sum_{n'=iSF}^{(i+1)SF}\hat{H}_u(n)\right)^2}{\sigma_\mu^2} = \frac{\frac{2E_t}{N_0}\left|\frac{1}{SF}\sum_{n'=iSF}^{(i+1)SF}\hat{H}_u(n)\right|^2}{1+\frac{1}{SF}\frac{E_t}{N_0}\sum_{\substack{u'=0\\ \neq u}}^{U-1}\left\{\frac{1}{SF}\sum_{n'=iSF}^{(i+1)SF-1}\left|\hat{H}_{u'}(n)\right|^2-\left|\frac{1}{SF}\sum_{n'=iSF}^{(i+1)SF-1}\hat{H}_{u'}(n)\right|^2\right\}}, \tag{18}$$

where n and n' are related by Eq. (2). The average BER can be numerically evaluated by averaging Eq. (17) over all possible values of $\{H_u(n); n = 0 \sim N-1, u = 0 \sim U-1\}$ as

$$P_b\left(\frac{E_t}{N_0}\right) = \int\cdots\int\frac{1}{2}erfc\left[\sqrt{\frac{1}{4}\gamma\left(\frac{E_t}{N_0},\{H_u(n)\}\right)}\right] p(\{H_u(n)\})\prod_{u,n}dH_u(n), \tag{19}$$

where $p(\{H_u(n)\})$ is the joint probability density function of $\{H_u(n); n = 0 \sim N-1, u = 0 \sim U-1\}$.

5. Numerical and Simulated Results

We assume MC-CDMA uplink with $N = 256$, $N_g = 32$, and QPSK data-modulation. In this paper, the channel is assumed to be composed of several clusters of propagation paths [10]. For the given total number L of paths, each cluster consists of exponentially decaying L/M paths, where M is the number of clusters and L/M is an integer. We consider M=1 and 2 as depicted in Figs. 5(a) and 5(b). The channel power delay profile $\Omega(\tau)$ for this channel model is given by

$$\Omega(\tau) = \Omega_0\sum_{l=0}^{L-1}\alpha^{-(l \bmod L/M)}\delta(\tau-\tau_l), \tag{20}$$

where α is the decay factor and $\Omega_0 = (1/M)(1-\alpha^{-1})/(1-\alpha^{-L/M})$. For pre-equalization transmission, the transmit timing control is necessary. When a practical timing control scheme is used, a timing error exists. The delay time $\tau_{u,l}$ of the uth user's lth path is expressed as $\tau_{u,l} = \Delta\tau_u + \tau_l$, where $\Delta\tau_u$ is the timing error and τ_l is the delay time difference between the 0th and lth paths. In this paper, we assume

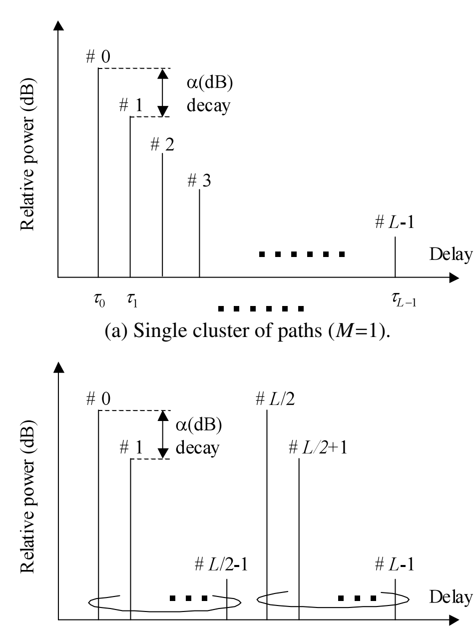

(a) Single cluster of paths (M=1).

(b) Two clusters of paths (M=2).

Fig. 5 Channel power delay profile model.

$\tau_l = l \cdot T_c$. It is assumed that uplink channel gains $\{H_u(n)\}$ can be perfectly estimated using the corresponding downlink channel.

We evaluate, by Monte Carlo numerical computation method, the theoretical BER performance of MC-CDMA uplink with GMMSE frequency-domain pre-equalization. Evaluation of the theoretical average BER performance is carried out by using the conditional BER expression obtained in Sect. 4 as follows. First, the complex path gains $\{\xi_{u,l}(t);\, u = 0 \sim U-1 \text{ and } l = 0 \sim L-1\}$ are generated, and $\{H_u(n);\, n = 0 \sim N-1,\, u = 0 \sim U-1\}$ are computed using Eq. (7) to obtain the pre-equalization weights using Eq. (11). Subsequently, the conditional BER with frequency-interleaving is calculated using Eq. (17) for the given E_t/N_0 and $\{H_u(n)\}$. By repeating the above procedure, the theoretical average BER expressed by Eq. (19) is obtained.

Also evaluated here is the computer-simulated BER performance. BER evaluation by the computer simulation is carried out as follows. At a transmitter, QPSK data-modulated sequence is generated (in Sect. 5.4, 16QAM is also considered) and spread by an orthogonal spreading sequence and a scramble sequence. The spread chip sequence in the frequency-domain is applied to frequency-interleaving and pre-equalized by using $\{H_u(n);\, u = 0 \sim U-1\}$, which are generated as in the theoretical evaluation. Then, after performing IFFT and insertion of GI, the pre-equalized MC-CDMA symbol sequence is obtained. They go through frequency-selective fading channels. At a receiver, after GI removal, frequency-deinterleaving and FFT is applied to get the time-domain sequence for despreading. Then, despreading is carried out to obtain the decision variables for QPSK data-demodulation. The recovered QPSK symbol sequence is compared with the transmitted symbol sequence to measure the number of bit errors. The above procedure is repeated sufficient number of times to obtain the average BER. We assume ideal transmit timing control ($\Delta\tau_u$=0) unless otherwise stated. The impact of timing error is discussed in Sect. 5.7.

5.1 Optimum x

The BER performance of MC-CDMA depends on the power delay profile shape. Figure 6 shows the dependency of the BER on the values of the decay factor α and the number M of path clusters when U=SF=64 for M=1 and 2. The theoretical average BER curves are plotted with solid lines. The simulated results are plotted as well in the same figure. The channel frequency-selectivity is a function of α; it is the strongest when α=0 dB and becomes weaker as α increases ($\alpha=\infty$ corresponds to the M-path channel). The optimum value of x that minimizes the BER for the given E_t/N_0 is dependent on α and M. It is seen from Fig. 6 that strictly speaking, the optimum x depends on α and M. For both M=1 and 2, the optimum x is around 0.6 when α=0 dB and increases as α increases; however, we can see a broad optimum x and the use of x=0.7 gives overall the minimum BER. In the following sections, we consider the single cluster case (M=1) only and use x=0.7.

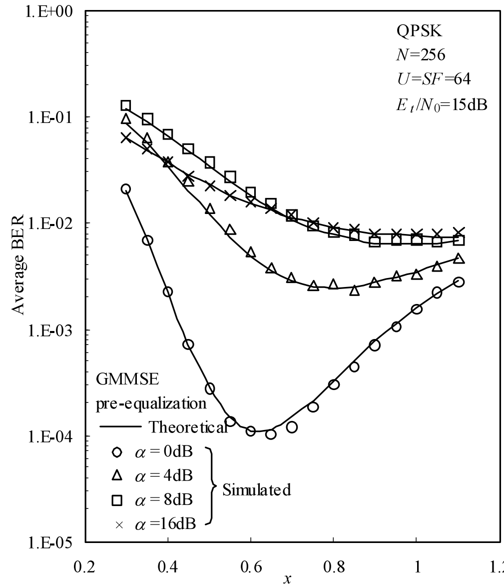

(a) Single cluster of paths (M=1).

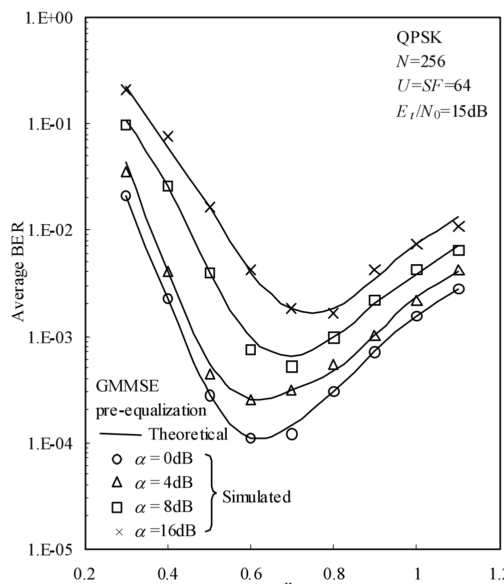

(b) Two clusters of paths (M=2).

Fig. 6 Impact of equalization target x.

5.2 Effect of Frequency-Interleaving

In MC-CDMA, as the spreading factor SF decreases, the frequency-diversity gain reduces and hence, the BER performance degrades if frequency interleaving is not used. This is because the subcarriers carrying the same data symbol tend to suffer similar fading. However by using the frequency interleaving, subcarriers carrying the same data symbol are separated each other so that they experience independent fading irrespective of SF. Hence, the BER performance using frequency interleaving may not be sensitive to the value of SF. The theoretical average BER performances of

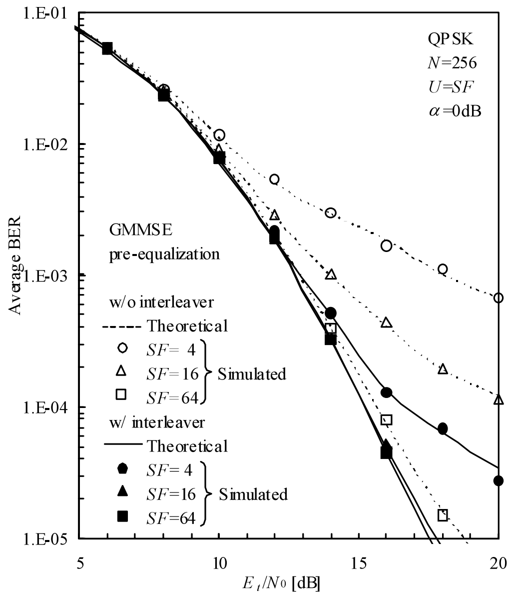

Fig. 7 Effect of frequency-interleaving.

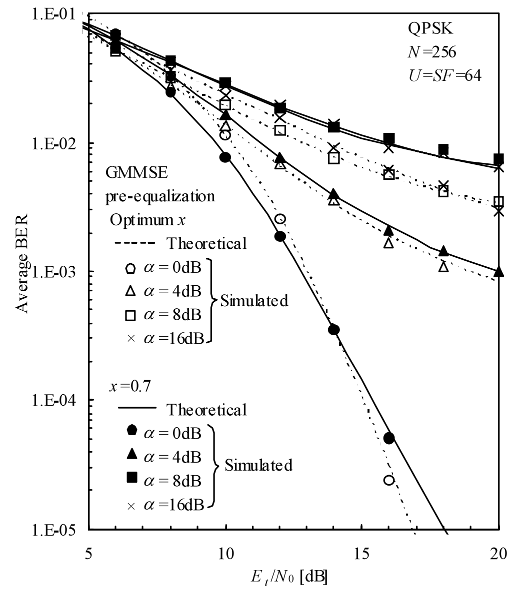

Fig. 8 Impact of decay factor α.

GMMSE frequency-domain pre-equalization (x=0.7) with and without frequency-interleaving are plotted in Fig. 7 for U/SF=1 (full load case) when SF=4, 16 and 64, as a function of E_t/N_0. Also plotted in Fig. 7 are the computer-simulated results to show that theoretical and simulation results agree well. Without frequency-interleaving, the BER performance depends on *SF* and degrades as *SF* becomes smaller due to less frequency-diversity gain. However, as was expected, with frequency-interleaving, the BER performance is almost insensitive to *SF* owing to larger frequency-diversity gain.

5.3 Impact of Decay Factor α

The theoretical average BER performances of GMMSE frequency-domain pre-equalization with x=0.7 are plotted by the solid lines as a parameter of α in Fig. 8. Also plotted in Fig. 8 are the simulated results. When α becomes larger, since frequency-selectivity becomes weaker, frequency-diversity gain is less, resulting in the degradation of the BER performance.

As was already described, the exact optimum value of x depends on α. The theoretical average BER performances with the exact optimum x for various values of α are plotted as the dashed lines in Fig. 8 for comparison. When α=0 dB (strong frequency-selectivity), the BER performance with x=0.7 is almost the same as with the exact optimum value of x=0.6. When α=8 dB (weak frequency-selectivity), the BER performance with x=0.7 is only slightly worse than with the exact optimum value of x=1.0. Therefore, x=0.7 can be used irrespective of α.

5.4 Comparison with MMSE Equalization Reception

The theoretical average BER performance curves and the simulated BERs of GMMSE pre-equalization (x=0.7) are plotted with U as a parameter in Fig. 9(a) for QPSK data-modulation and in Fig. 9(b) for 16QAM data-modulation (for the sake of brevity, the BER analysis for 16QAM data-modulation is omitted in this paper). For comparison, the simulated results of MMSE frequency-domain equalization reception are plotted (instead of using pre-equalization at the mobile station transmitter, MMSE equalization reception is used at the base station receiver).

First, we consider the case of QPSK data-modulation. When U=1, since there is no MAI, a good BER performance is obtained by using MMSE equalization reception. However, when the number of users is large (U=16, 64), the BER performance with MMSE equalization reception significantly degrades since a large MAI is produced. On the other hand, GMMSE pre-equalization provides much better BER performance than MMSE equalization reception. When $U > 4$, the required E_b/N_0 for BER=10^{-3} is smaller with GMMSE pre-equalization than with MMSE equalization reception.

When higher-level modulation is used, the MAI severely degrades the BER performance. It can be seen from Fig. 9(b) that with MMSE equalization reception, a large BER floor is seen even when U=4. On the other hand, no error floor is seen with GMMSE pre-equalization when U=4 and 16.

5.5 Impact of Number U of Users

The theoretical average BER performances with GMMSE pre-equalization are plotted for SF=64 with the number U of users as a parameter in Fig. 10. Also plotted in Fig. 10 are simulated results. When U=4, the BER performance is almost the same as when U=1. When U=16, the E_t/N_0 degradation for BER=10^{-3} from the single-user case is only about

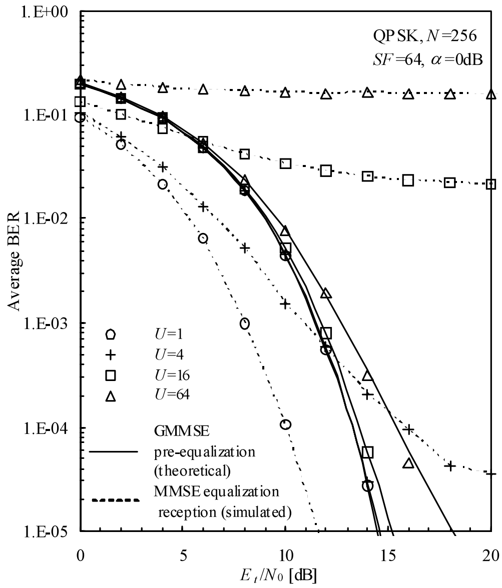

(a) QPSK

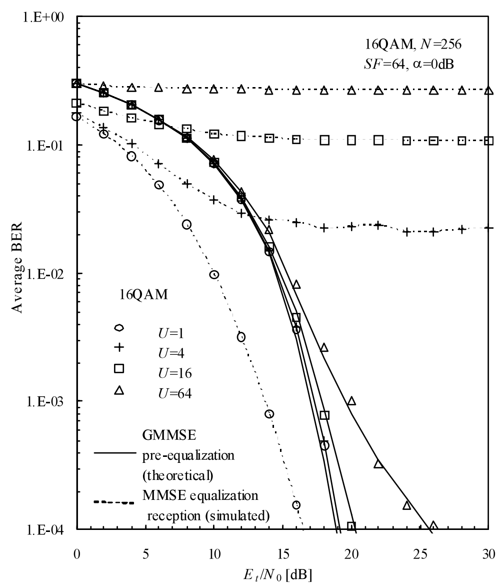

(b) 16QAM

Fig. 9 Performance comparison between GMMSE pre-equalization and MMSE equalization reception.

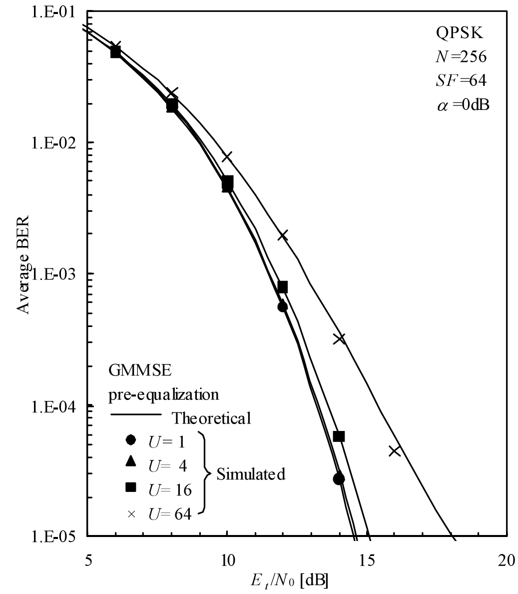

Fig. 10 Impact of U.

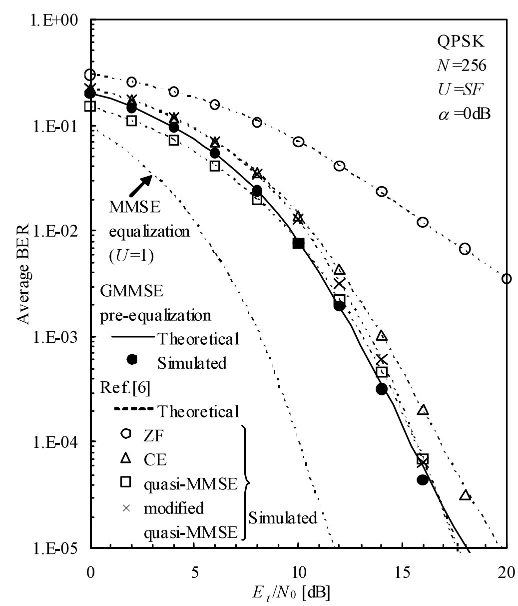

Fig. 11 Comparison of various frequency-domain pre-equalization techniques.

0.5 dB. This is because by using GMMSE pre-equalization, the use of x=0.7 can make the equivalent channel gain almost stable (i.e., the channel can be close to frequency-nonselective channel) by allowing the increased power loss. When U=64, the E_t/N_0 degradation for BER=10^{-3} from the single-user case is only about 2 dB.

5.6 Comparison with Various Frequency-Domain Pre-Equalization Techniques [6]

We compare the BER performance achievable with GMMSE pre-equalization with those of MMSE, quasi-MMSE, modified quasi-MMSE, ZF and controlled equalization (CE) frequency-domain pre-equalization techniques presented in Ref. [6] (their pre-equalization weights are shown in Appendix B). The BER performance comparison is shown in Fig. 11 for U=SF=64. We found by our computer simulation that the optimum values for the threshold $a_{threshold}$ of CE and λ of modified quasi-MMSE, which minimize the required E_t/N_0 for BER=10^{-3}, are $a_{threshold}$=0.175 and λ=0.013. They are used for BER evaluations of CE and modified quasi-MMSE in this paper. Among various pre-equalization techniques of Ref. [6], quasi-MMSE provides the best performance. Although GMMSE is inferior to quasi-MMSE in low E_t/N_0 regions (i.e., E_t/N_0 < 11 dB), it can provide almost the same or slightly better performance

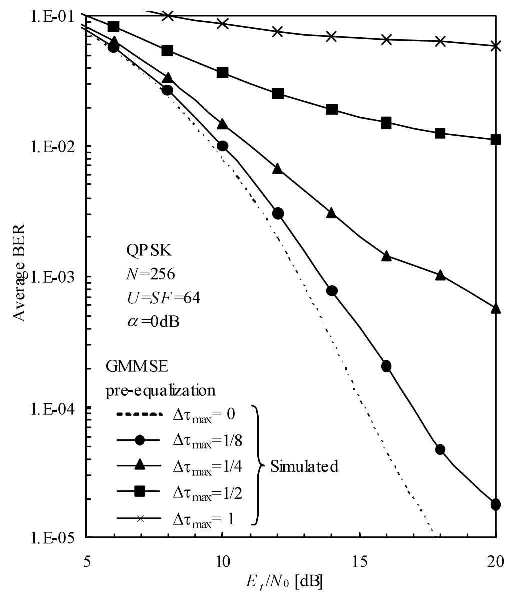

Fig. 12 Impact of transmit timing error.

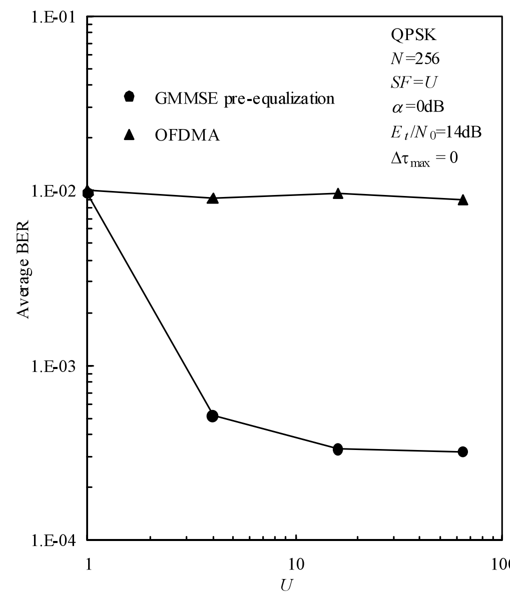

Fig. 13 Comparison with OFDMA.

than quasi-MMSE in large E_t/N_0 regions.

5.7 Impact of Transmit Timing Error

So far, we have assumed the ideal transmit power control (i.e., $\Delta\tau_u$=0 and all the received MC-CDMA signals transmitted from different users are time-synchronous). However, for a practical transmit timing control scheme, the timing error exists in the received signals. Here, we evaluate how the timing error impacts the achievable BER performance. Each user's transmit timing error is assumed to be independent and uniformly distributed over $[-\Delta\tau_{max} \cdot T_c/2, +\Delta\tau_{max} \cdot T_c/2]$. Figure 12 plots the BER performance of GMMSE frequency-domain pre-equalization as a function of E_t/N_0 with $\Delta\tau_{max}$ as a parameter. It is seen that the BER performance is sensitive to $\Delta\tau_{max}$ and a high BER floor is produced when $\Delta\tau_{max} > 1/2$. To suppress the E_t/N_0 degradation for BER=10^{-3} from the ideal transmit timing control case within 1 dB, the timing control error should be kept within $\Delta\tau_{max}$=1/8.

5.8 Comparison with OFDMA

Orthogonal frequency division multiplexing access (OFDMA) has been considered to be a promising access scheme, that assigns a different set of subcarriers to different users in order to avoid the MAI [11]; a total of $256/U$ subcarriers, from the $256(u/U)$-the subcarrier to the $(256(u+1)/U-1)$th subcarrier, is assigned to the u-th user. For performance comparison of GMMSE pre-equalization and OFDMA, the BER at E_t/N_0=14 dB is plotted as a function of U in Fig. 13. We assume the same data rate for all U users. In MC-CDMA using GMMSE pre-equalization, SF=U is assumed. It is seen in Fig. 13 that OFDMA achieves the same BER performance regardless of U, since the MAI can be completely avoided. On the other hand, when GMMSE pre-equalization is used, the BER decreases as U increases. GMMSE pre-equalization provides better BER performance than OFDMA. This is because the increased frequency diversity effect owing to increased spreading factor (SF=U) offsets the increased MAI produced by the orthogonality distortion.

6. Conclusion

In this paper, generalized minimum mean square error (GMMSE) frequency-domain pre-equalization was presented for MC-CDMA/TDD uplink (mobile-to-base station). GMMSE pre-equalization minimizes the error between the equivalent channel gain and the pre-equalization target x under the transmit power constraint. The theoretical analysis of conditional BER was presented. The theoretical average BER performance was evaluated by Monte Carlo numerical computation method using the derived conditional BER expression and confirmed by the computer simulation.

Since the optimum equalization target x depends on the channel power delay profile shape, the measurement of the power delay profile shape is necessary to always set the value of x to the optimum; however, it was found from the theoretical and simulation results that the BER performance can be improved by setting x=0.7 for two power delay profile shapes: one is 16-path exponentially decaying profile and the other is the two clusters of paths, each has 8-path exponentially decaying profile. It was also found that the BER performance with frequency-interleaving is almost insensitive to the spreading factor SF owing to larger frequency diversity effect. GMMSE pre-equalization was also compared with various pre-equalization techniques presented in Ref. [6]. GMMSE pre-equalization was found to achieve almost the same BER performance as the quasi-MMSE pre-equalization technique of Ref. [6].

Also discussed in this paper was the impact of transmit timing control error on the achievable BER performance. When the timing error is present, the orthogonality among different users is destroyed even when the pre-equalization technique is utilized, and the performance degrades. It was found that the timing error needs to be controlled within $\Delta\tau_{max}$=1/8, otherwise the performance significantly degrades. Therefore, the transmit timing control is a very important technical issue for a future study.

We showed that the GMMSE pre-equalization can achieve better BER performance than OFDMA in a multiuser environment. However, only uncoded transmission was considered in this paper. When coding is applied, OFDMA can achieve a large coding gain due to better frequency interleaving effect than MC-CDMA [12]. The performance comparison between GMMSE pre-equalization and OFDMA for the coded case is an interesting future study.

When using TDD, channel estimate for the downlink channel can be used for the uplink channel. In this paper, ideal channel estimation was assumed. However, there is in fact channel estimation error. Moreover, since there is a time lag between the downlink and uplink slots, the channel estimation error for the uplink pre-equalization further increases. The impact of channel estimation error is also left as an important future study.

References

[1] W.C. Jakes, Jr., ed., Microwave mobile communications, Wiley, New York, 1974.
[2] S. Hara and R. Prasad, "Overview of multicarrier CDMA," IEEE Commun. Mag., vol.35, no.12, pp.126–133, Dec. 1997.
[3] H. Atarashi, S. Abeta, and M. Sawahashi, "Variable spreading factor-orthogonal frequency and code division multiplexing (VSF-OFCDM) for broadband packet wireless access," IEICE Trans. Commun., vol.E86-B, no.1, pp.291–299, Jan. 2003.
[4] T. Sao and F. Adachi, "Comparative study of various frequency equalization techniques for downlink of a wireless OFDM-CDMA system," IEICE Trans. Commun., vol.E86-B, no.1, pp.352–363, Jan. 2003.
[5] S. Verdu, Multiuser detection, Cambridge University Press, 1998.
[6] I. Cosovic, M. Schnell, and A. Springer, "On the performance of different channel pre-compensation techniques for uplink time division duplex MC-CDMA," Proc. IEEE Vehicular Technology Conference (VTC'03 Fall), vol.2, pp.857–861, Oct. 2003.
[7] R. Esmalizadeh, M. Nakagawa, and A. Jones, "TDD-CDMA for the 4th generation of wireless communications," IEEE Wireless Commun. Mag., vol.10, no.4, pp.8–15, Aug. 2003.
[8] S. Haykin, Adaptive filter theory, 3rd ed., Prentice Hall, 1996.
[9] J.G. Proakis, Digital communications, 3rd ed., McGraw-Hill, 1995.
[10] S. Abeta, H. Atarashi, M. Sawahashi, and F. Adachi, "Performance of coherent multi-carrier/DS-CDMA and MC-CDMA for broadband packet wireless access," IEICE Trans. Commun., vol.E84-B, no.3, pp.406–414, March 2001.
[11] H. Sari and G. Karam, "Orthogonal frequency-division multiple access and its application to CATV networks," European Trans. Telecom. & Related Tech. (ETT), vol.9, no.6, pp.507–516, Nov./Dec. 1998.
[12] D. Garg and F. Adachi, "Diversity-coding-orthogonality trada-off for coded MC-CDMA with high level modulation," IEICE Trans. Commun., vol.E88-B, no.1, pp.76–83, Jan. 2005.

Appendix A: Derivation of σ^2_{MAI} and σ^2_{AWGN}

$\mu_{MAI}(i)$ of Eq. (14) can be rewritten as

$$\mu_{MAI}(i) = \sqrt{\frac{2E_t}{T_c}\frac{1}{SF\cdot N}}\sum_{\substack{v=0\\ \neq u}}^{U-1} d_v(i) \times\left[\frac{1}{SF}\sum_{n'=iSF}^{(i+1)SF-1}\left\{\hat{H}_v(n)-\bar{H}_v(i)+\bar{H}_v(i)\right\} c_v(n' \bmod SF)c_u^*(n' \bmod SF)\right], \quad (\text{A}\cdot 1)$$

where $n=(n' \bmod SF)\times SF+\left\lfloor\frac{n'}{SF}\right\rfloor$ (see Eq. (2)) and $\bar{H}_v(i)$ is defined as

$$\bar{H}_v(i)=\frac{1}{SF}\sum_{n'=iSF}^{(i+1)SF-1}\hat{H}_v(n). \quad (\text{A}\cdot 2)$$

Since the orthogonal spreading sequences are used,

$$\sum_{n'=iSF}^{(i+1)SF-1}\sum_{\substack{v=0\\ \neq u}}^{U-1} c_v(n' \bmod SF)c_u^*(n' \bmod SF)=0, \quad (\text{A}\cdot 3)$$

and hence, Eq. (A· 1) can be rewritten as

$$\mu_{MAI}(i) = \sqrt{\frac{2E_t}{T_c}\frac{1}{SF\cdot N}}\sum_{\substack{v=0\\ \neq u}}^{U-1} d_v(i) \times\left[\frac{1}{SF}\sum_{n'=iSF}^{(i+1)SF-1}\left\{\hat{H}_v(n)-\bar{H}_v(i)\right\} c_v(n' \bmod SF)c_u^*(n' \bmod SF)\right]. \quad (\text{A}\cdot 4)$$

Using Eq. (A· 4), the variance $2\sigma^2_{MAI}$ of $\mu_{MAI}(i)$ is given by

$$\begin{aligned}2\sigma^2_{MAI} &= E\left[|\mu_{MAI}(i)|^2\right]\\ &= \frac{2E_t}{T_c}\frac{1}{SF^3}\frac{1}{N}\sum_{\substack{v=0\\ \neq u}}^{U-1}\sum_{\substack{w=0\\ \neq u}}^{U-1} d_v(i)d_w^*(i)\sum_{n'=iSF}^{(i+1)SF-1}\sum_{m'=iSF}^{(i+1)SF-1}\\ &\left\{\begin{array}{l}\left(\hat{H}_v(n)-\bar{H}_v(i)\right)\left(\hat{H}_w(m)-\bar{H}_w(i)\right)^* c_v(n' \bmod SF)\\ \times c_u^*(n' \bmod SF)c_w^*(m' \bmod SF)c_u(m' \bmod SF)\end{array}\right\}.\end{aligned} \quad (\text{A}\cdot 5)$$

Since $E\left[d_v(i)d_w^*(i)\right]=0$ if $v\neq w$ and $|d_v(i)|=1$, Eq. (A· 5) becomes

$$2\sigma^2_{MAI} = \frac{2E_t}{T_c}\frac{1}{SF^3}\frac{1}{N}\sum_{\substack{v=0\\ \neq u}}^{U-1}\sum_{n'=iSF}^{(i+1)SF-1}\left|\hat{H}_v(n')-\bar{H}_v(i)\right|^2$$
$$+\frac{2E_t}{T_c}\frac{1}{SF^3}\frac{1}{N}\sum_{\substack{v=iSF\\ \neq u}}^{(i+1)SF-1}\sum_{n'=iSF}^{(i+1)SF-1}\sum_{\substack{m'=iSF\\ \neq n'}}^{(i+1)SF-1}$$

$$\left[\begin{array}{l}\left\{\hat{H}_v(n)-\bar{H}_v(i)\right\}\left\{\hat{H}_w(m)-\bar{H}_w(i)\right\}^* c_v(n' \bmod SF)\\ \times c_u^*(n' \bmod SF)c_w^*(m' \bmod SF)c_u(m' \bmod SF)\end{array}\right]. \tag{A·6}$$

Since a spreading code takes the value of 1 or −1 with equal probability, we have, from the law of large numbers [9],

$$\sum_v c_v(n' \bmod SF)c_u^*(n' \bmod SF) \times c_w^*(m' \bmod SF)c_u(m' \bmod SF) \approx 0 \tag{A·7}$$

for large values of U and SF. Therefore, the 2nd term of Eq. (A·6) can be neglected and $2\sigma^2_{MAI}$ can be approximated as

$$2\sigma^2_{MAI} \approx \frac{2E_t}{T_c}\frac{1}{SF^2}\frac{1}{N}\sum_{\substack{v=0\\ \neq u}}^{U-1}\left(\frac{1}{SF}\sum_{n'=iSF}^{(i+1)SF-1}\left|\hat{H}_v(n)-\bar{H}_v(i)\right|^2\right). \tag{A·8}$$

Next, the variance $2\sigma^2_{AWGN}$ of $\mu_{AWGN}(i)$ is obtained. $2\sigma^2_{AWGN}$ is given by

$$2\sigma^2_{AWGN} = \frac{1}{SF^2}\sum_{n'=iSF}^{(i+1)SF}\sum_{m'=iSF}^{(i+1)SF-1} \{c_u(n' \bmod SF)c_u^*(m' \bmod SF)E\left[\Pi(n)\Pi^*(m)\right]\}. \tag{A·9}$$

Since

$$E\left[\Pi(n)\Pi^*(m)\right] = \frac{2N_0}{NT_c}\delta(n-m), \tag{A·10}$$

we have

$$2\sigma^2_{AWGN} = \frac{1}{SF}\frac{2N_0}{NT_c}. \tag{A·11}$$

Appendix B: Various Frequency-Domain Pre-Equalization Techniques

Various frequency-domain pre-equalization techniques presented in Ref. [6] are reviewed below.

(1) MMSE

MMSE pre-equalization minimizes the mean-square error between the transmitted nth subcarrier component $S_u(n)$ and the received nth subcarrier component $R_u(n)$ under the transmit power constraint. Pre-equalization weight is given by

$$w_u(n) = \frac{H_u^*(n)}{|H_u(n)|^2+\lambda_u}, \tag{A·12}$$

where λ_u satisfies

$$\sum_{n=0}^{N-1}\frac{|H_u(n)|^2}{\left(|H_u(n)|^2+\lambda_u\right)^2} = N, \tag{A·13}$$

and is obtained by numerical computation. Note that MMSE pre-equalization is equivalent to GMMSE pre-equalization using x=1.

(2) quasi-MMSE

MMSE per subcarrier equalization for the downlink MC-CDMA transmission is slightly modified under the power constraint and applied to uplink transmission [6]. This solution is termed Quasi-MMSE pre-equalization, since it does not represent the real MMSE uplink pre-equalization technique. Pre-equalization weight is given by

$$w_u(n) = \frac{H_u^*(n)}{|H_u(n)|^2+\frac{SF}{(E_t/N_0)(U-1)}} \times \sqrt{\frac{N}{\sum_{n=0}^{N-1}\frac{|H_u(n)|^2}{\left(|H_u(n)|^2+\frac{SF}{(E_t/N_0)(U-1)}\right)^2}}}. \tag{A·14}$$

(3) modified quasi-MMSE

Modified quasi-MMSE pre-equalization is a pre-equalization, which replaces the 2nd term of the denominator of Eq. (A·14) by the variable λ. Pre-equalization weight is given by

$$w_u(n) = \frac{H_u^*(n)}{|H_u(n)|^2+\lambda}\sqrt{\frac{N}{\sum_{n=0}^{N-1}\frac{|H_u(n)|^2}{\left(|H_u(n)|^2+\lambda\right)^2}}}, \tag{A·15}$$

where the optimum λ can be found by numerical computation.

(4) ZF

ZF pre-equalization weight is given by

$$w_u(n) = \frac{1}{H_u(n)}\sqrt{\frac{N}{\sum_{n=0}^{N-1}|H_u(n)|^{-2}}}. \tag{A·16}$$

Since $w_u(n)$ is inversely proportional to the channel gain, the equivalent channel gain $H_u(n)w_u(n)$ becomes unity and can completely eliminate the MAI. However, the weight becomes fairly large for the subcarrier where the channel gain drops, thereby producing a large power loss in the received signal under the transmit power constraint. Hence, the BER performance degrades due to the AWGN.

(5) CE

CE uses ZF at the subcarrier where channel gain is larger than $a_{threshold}$, otherwise EGC is used. Pre-equalization weight is given by

$$w_u(n) = \begin{cases}\dfrac{1}{H_u(n)}\sqrt{\dfrac{N}{\sum_{n=0}^{N-1}|H_u(n)|^{-2}}}, & \text{if } |H_u(n')| \geq a_{threshold}\\[2ex] \dfrac{H_u^*(n)}{|H_u(n)|}, & \text{otherwise}\end{cases}. \tag{A·17}$$

Satoshi Abe received his B.S. and M.S. degrees in communications engineering from Tohoku University, Sendai, Japan, in 2003 and 2005, respectively. His research topic was the frequency-domain pre-equalization techniques for next generation wireless communication systems. Since April 2005, he has been with KDDI Corp., Tokyo, Japan, where he is involved in the development of CDMA2000 1x EV-DO at the Mobile Network Development Department.

Shinsuke Takaoka received his B.S. and M.S. degrees in communications engineering from Tohoku University, Sendai, Japan, in 2001 and 2003, respectively. Currently, he is a graduate student at the Department of Electrical and Communications Engineering, Tohoku University. His research interests include digital signal transmission techniques, especially for mobile communication systems.

Hiromichi Tomeba received his B.S. degree in communications engineering from Tohoku University, Sendai, Japan, in 2004. Currently he is a graduate student at the department of Electrical and Communications Engineering, Graduate School of Engineering, Tohoku University. His research interests include frequency-domain pre-equalization and antenna diversity techniques for mobile communication systems.

Fumiyuki Adachi received his B.S. and Dr. Eng. Degrees in electrical engineering from Tohoku University, Sendai, Japan, in 1973 and 1984, respectively. In April 1973, he joined the electrical Communications Laboratories of Nippon Telegraph & Telephone Corporation (now NTT) and conducted various types of research related to digital cellular mobile communications. From July 1992 to December 1999, he was with NTT Mobile Communications Network, Inc. (now NTT DoCoMo, Inc.), where he led a research group on wideband/broadband CDMA wireless access for IMT-2000 and beyond. Since January 2000, he has been with Tohoku University, Sendai, Japan, where he is a Professor of Electrical and Communication Engineering at Graduate School of Engineering. His research interests are in CDMA and TDMA wireless access techniques, CDMA spreading code design, Rake receiver, transmit/receive antenna diversity, adaptive antenna array, bandwidth-efficient digital modulation, and channel coding, with particular application to broadband wireless communication systems. From October 1984 to September 1985, he was a United Kingdom SERC Visiting Research Fellow in the Department of Electrical Engineering and Electronics at Liverpool University. He was a co-recipient of the IEICE Transactions best paper of the year award 1996 and again 1998. He is an IEEE Fellow and was a co-recipient of the IEEE Vehicular Technology Transactions best paper of the year award 1980 and again 1990 and also a recipient of Avant Garde award 2000.